

A Framework for Controllable Multi-objective Learning with Annealed Stein Variational Hypernetworks

Minh-Duc Nguyen¹ and Dung D. Le^{1*}

¹College of Engineering and Computer Science, VinUniversity,
Hanoi, Vietnam.

*Corresponding author(s). E-mail(s): dung.ld@vinuni.edu.vn;
Contributing authors: duc.nm2@vinuni.edu.vn;

Abstract

Pareto Set Learning (PSL) is popular as an efficient approach to obtaining the complete optimal solution in Multi-objective Learning (MOL). A set of optimal solutions approximates the Pareto set, and its mapping is a set of dense points in the Pareto front in objective space. However, some current methods face a challenge: how to make the Pareto solution is diverse while maximizing the hypervolume value. In this paper, we propose a novel method to address this challenge, which employs Stein Variational Gradient Descent (SVGD) to approximate the entire Pareto set. SVGD pushes a set of particles towards the Pareto set by applying a form of functional gradient descent, which helps to converge and diversify optimal solutions. Additionally, we employ diverse gradient direction strategies to thoroughly investigate a unified framework for SVGD in multi-objective optimization and adapt this framework with an annealing schedule to promote stability. We introduce our method, SVH-MOL, and validate its effectiveness through extensive experiments on multi-objective problems and multi-task learning, demonstrating its superior performance.

Keywords: Multi-objective Optimization, Stein Variational Gradient Descent, Pareto Front Learning, Hypernet

1 Introduction

Multi-objective optimization (MOO) is a critical area of research in the field of optimization, focusing on problems that involve multiple conflicting objectives. Unlike traditional single-objective optimization, where the goal is to find a single optimal solution, MOO seeks to find a set of solutions that represent the trade-offs between the different objectives. MOO has been successfully applied across diverse fields, from energy system design [Marler and Arora \(2004\)](#) to healthcare treatment planning [Craft et al. \(2006\)](#), demonstrating its versatility in balancing conflicting objectives. In machine learning, multi-objective problems play a significant role in various applications, including recommender systems [Milojkovic et al. \(2019\)](#); [Jannach \(2022\)](#); [Zaizi et al. \(2023\)](#), where they help balance multiple conflicting criteria, and multi-task learning [Sener and Koltun \(2018\)](#); [Crawshaw \(2020\)](#), where they optimize performance across multiple related tasks simultaneously. Furthermore, addressing multi-objective problems in real-world scenarios can be computationally demanding [Lin et al. \(2022\)](#), particularly in high-dimensional settings [Nguyen and Tran \(2024\)](#), as it involves assessing multiple conflicting objectives, which increases computational costs.

A common method for addressing multi-objective problems is to transform them into a single-objective problem using scalarization. This method assigns weights to each objective, representing their trade-offs and relative importance. The optimization process then finds a single solution corresponding to a specific weight vector. Thus, for each weight vector, we obtain only a single solution within a specific sub-region of the objective space, which is defined by the chosen weighting scheme and the trade-offs between objectives. This subregion represents a portion of the Pareto front that aligns with the given weight vector. As a result, the disadvantage is how choose the desired weight. MOEA/D [Zhang and Li \(2007\)](#) (Multi-Objective Evolutionary Algorithm based on Decomposition) is a widely used multi-objective optimization algorithm that decomposes a multi-objective problem into several single-objective subproblems and optimizes them simultaneously. MOEA/D enhances solution diversity by decomposing the problem into multiple subproblems, allowing for a more distributed exploration of the solution space.

The current survey [Chen et al. \(2025\)](#) has classified MOO algorithms for multi-task learning into three approaches following the number of optimal solutions:

- Finding a single Pareto solution: A single optimal solution is obtained, representing a solution with the contribution of each objective appropriately, ensuring that the final solution is not overly biased toward any particular objective. This balance is typically achieved through techniques such as loss balancing [Liu et al. \(2019\)](#); [Kendall et al. \(2018\)](#); [Lin et al. \(2024\)](#) and gradient-based adjustments [Sener and Koltun \(2018\)](#); [Chen et al. \(2018\)](#); [Yu et al. \(2020\)](#), which dynamically regulate the influence of each objective during the optimization process.
- Finding a finite set of Pareto solutions: This approach provides users with a diverse set of options to choose from based on their specific requirements. Generally, preference vector-based methods are used to divide the problem into subproblems, where each solution is found by optimizing a specific subproblem defined by a preference vector. Furthermore, methods such as Pareto Multi-Task Learning (PMTL) [Lin](#)

et al. (2019) leverage this strategy by evenly distributing preference vectors across the objective space to capture different trade-off regions. Alternatively, algorithms like Exact Pareto Optimal (EPO) Mahapatra and Rajan (2020) Search use techniques such as gradient descent with controlled ascent to precisely navigate the Pareto front and locate solutions that exactly satisfy the user-specified preferences.

- Finding an infinite set of Pareto solutions: This approach seeks to compute the complete Pareto front—that is, a continuum of Pareto optimal solutions that are continuously and densely distributed in the objective space. The hypernetwork-based method Navon et al. (2020); Hoang et al. (2023) obtains a good Pareto front by mapping the preference vector space directly to the optimal solution space. Moreover, this hypernetwork-based framework significantly reduces the need for training multiple separate models for various preference settings. Instead, a single model can be employed to generate a diverse set of solutions, making it especially suitable for complex multi-task learning scenarios where balancing objectives is critical.

In our research, we investigate the third approach discussed in the context of Pareto set learning methods, which involves utilizing hypernetwork-based strategies. We observe that the current method faces a major challenge, which is that the Pareto set is difficult to diversify. In PHN-HVI Hoang et al. (2023), the authors leverage hypervolume maximization Deist et al. (2021) to derive the optimal solution while incorporating a penalty function to promote diversity among the resulting Pareto solutions. Using Hypervolume maximization as a gradient descent direction helps to find the optimal solution, but similar to MGDA, it tends to move towards a single optimal point. Therefore, in PHN-HVI, the incorporation of a penalty function promotes a more diverse spread of solutions along the Pareto front. However, this diversification can come at the cost of convergence precision, potentially steering the optimization process away from the most optimal points in the objective space.

To tackle this challenge, we propose a novel approach for efficiently learning the complete Pareto set while capturing its inherent diversity. Our method is inspired by the previous study MOO-SVGD Liu et al. (2021), which employs Stein Variational Gradient Descent (SVGD) Liu and Wang (2016) to approximate the Pareto set. However, MOO-SVGD results in a discrete set of solutions. In contrast, our approach is designed to learn a continuous representation of the Pareto front, ensuring that all possible trade-offs are effectively captured. Our framework, SVH-MOL, has the following contributions:

- Firstly, we introduce an innovative framework that integrates hypernetwork-based techniques with Stein Variational Gradient Descent for multi-objective learning.
- Secondly, we investigate several variations of the gradient descent algorithm within the SVGD framework to fully capture and optimize the capabilities of our approach. Additionally, we employ an annealing schedule to encourage diversity in the Pareto set.
- Thirdly, we evaluated our framework across a broad spectrum of applications, ranging from traditional multi-objective optimization (MOO) tasks to large-scale multi-task learning problems. In our experiments, we demonstrated that our

approach not only effectively captures the intricate trade-offs inherent in MOO scenarios but also scales robustly to complex, real-world multi-task settings.

2 Related Work

Multi-objective Optimisation (MOO)

MOO is a fundamental challenge in machine learning, where it aims to find a set of optimal solutions that each solution represents the best trade-off between multiple conflicting objectives. Evolutionary algorithms are popular to find a set of diverse Pareto optimal solutions in a single run, such as VEGA [Schaffer \(2014\)](#), NSGA-III [Deb and Jain \(2013\)](#). This approach often faces challenges in high-dimensional spaces and require significant computational resources. In contrast, gradient-based methods have emerged as more efficient alternatives, particularly in differentiable settings. This method leverages the gradients of the objective functions to guide the search toward Pareto-optimal solutions. Scalarization techniques, such as the weighted sum method [Yang \(2014\)](#) and the Tchebyshev method [Steuer and Choo \(1983\)](#), provide an efficient approach for transforming multiple objectives into a single aggregated objective, enabling the use of gradient-based optimization methods.

Pareto Set Learning (PSL).

PSL emerges as a proficient means of approximating the entire Pareto front; it employs a hypernetwork [Ha et al. \(2016\)](#) to learn a mapping between a preference vector and an optimal solution in a single training. Many studies proposed different gradient descent methods to optimize the combined-objective function, such as PHN-LS and PHN-EPO [Navon et al. \(2020\)](#). [Hoang et al. \(2023\)](#) use maximizing the hypervolume indicator to guide the search for the optimal region. One framework for controllable Pareto front learning employs the completed scalarization functions proposed by [Tuan et al. \(2024\)](#). PSL has been effectively applied to the optimization of multiple black-box functions [Lin et al. \(2022\)](#), where it can efficiently suggest the next experiment to conduct in a laboratory setting.

Stein Variational Gradient Descent (SVGD).

SVGD is a gradient method for approximating a target distribution, which was originally proposed for Bayesian inference [Liu and Wang \(2016\)](#). SVGD iteratively transports a set of particles to approximate a target distribution by minimizing the Kullback-Leibler (KL) divergence. However, [Zhao et al. \(2018\)](#) observes that particles of SVGD tend to collapse to modes of the target distribution, and this particle degeneracy phenomenon becomes more severe with higher dimensions. This issue was explained in this study [Ba et al. \(2021\)](#), the authors compared the SVGD update with the gradient descent on the maximum mean discrepancy (MMD). To address this challenge, [D'Angelo and Fortuin \(2021\)](#) employs an annealing schedule to solve the inability of the particles to escape from local modes and the inefficiency in reproducing the density of the different regions. Selecting an appropriate kernel remains a key

challenge, as the performance of the algorithm is highly dependent on the choice of kernel [Duncan et al. \(2023\)](#). Multiple-kernel learning (MKL) enables the combination of multiple kernels into a single, unified kernel, providing greater flexibility in the learning process [Ai et al. \(2023\)](#). In MOO, the first study MOO-SVGD [Liu et al. \(2021\)](#) adapted SVGD to profile the Pareto front while maintaining diversity, providing an efficient alternative to traditional methods.

3 Preliminaries

3.1 Multi-objective optimization

Multi-objective optimization (MOO) refers to the process of simultaneously optimizing two or more conflicting objectives subject to a set of constraints. Unlike single-objective optimization, where a unique optimal solution exists, MOO typically results in a set of optimal trade-offs known as the Pareto front.

Formally, a multi-objective optimization problem can be defined as:

$$\min_{x \in \mathcal{X}} \mathcal{F}(x) = \begin{bmatrix} f_1(x) \\ f_2(x) \\ \vdots \\ f_m(x) \end{bmatrix}, \quad (1)$$

where $\mathcal{F}(x) = [f_1(x), f_2(x), \dots, f_m(x)]^T$ represents the m objective functions, $\mathcal{F}(\cdot) : \mathcal{X} \rightarrow \mathcal{Y} \subset \mathbb{R}^m$ and $\mathcal{X} \subset \mathbb{R}^n$ denotes the feasible decision space.

Definition 1 (Dominance) A solution x^a dominates x^b if: $f_j(x^a) \leq f_j(x^b), \forall j$ and $f_j(x^a) \neq f_j(x^b)$ for at least one j . Denote $\mathcal{F}(x^a) \prec \mathcal{F}(x^b)$.

Definition 2 (Pareto Optimal Solution) A solution x^a is considered Pareto optimal if no other solution x^b exists such that: $\mathcal{F}(x^b) \preceq \mathcal{F}(x^a)$.

Definition 3 (Weakly Pareto Optimal Solution) A solution x^a is called weakly Pareto optimal if there is no solution x^b such that: $\mathcal{F}(x^b) \prec \mathcal{F}(x^a)$.

Definition 4 (Pareto Set/Pareto Front) The set of all Pareto optimal solutions is referred to as the Pareto set, denoted as X_E , and the corresponding objective space representation is known as the Pareto front, given by: $P_F = \mathcal{F}(X_E)$.

3.2 Pareto Set Learning

Pareto Set Learning (PSL) offers an efficient approach to obtaining the entire Pareto set in a single training phase, contrasting with traditional methods that require varying hyperparameters to approximate only a few Pareto-optimal points. PSL employs a hypernetwork [Ha et al. \(2016\)](#) to generate a diverse set of candidate solutions. During training, the hypernetwork's parameters are optimized by directly minimizing

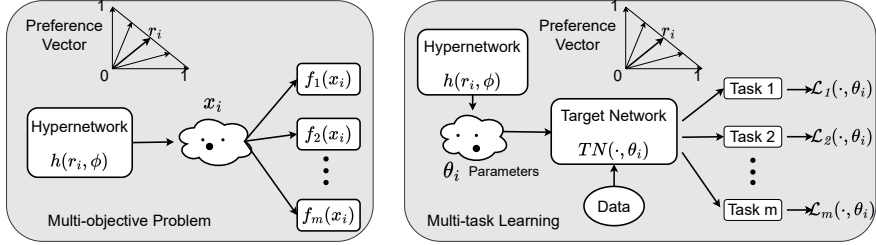


Fig. 1 Pareto Set Learning Framework

the multi-objective optimization (MOO) objective. Consequently, the trained hypernetwork produces a dense set of solutions that closely approximate the true Pareto front.

In our study, PSL is applied to multi-objective optimization, where the decision variable x is generated by the hypernetwork. Additionally, in the context of multi-task learning, the hypernetwork is designed to output the full set of parameters for the target network responsible for solving the main tasks (Figure 1).

In multi-objective learning, our approach is based on a set of predefined preference vectors as a trade-off between the conflicting objectives, which is the input for the hypernetwork. We formulate the optimize process as:

$$\begin{aligned} \phi^* &= \arg \min_{\phi} \mathbb{E}_{r \sim \text{Dir}(\alpha)} s(\mathcal{F}(\mathbf{x}_r), r) \\ \text{s.t. } \mathbf{x}_r &= \mathbf{h}(r, \phi^*) \in X_E, \mathbf{h}(\mathcal{P}, \phi^*) \equiv X_E \end{aligned} \quad (2)$$

where Hypernetwork $h : \mathcal{P} \times \mathbb{R}^q \rightarrow \mathbb{R}^n$, q is the number of parameters of hypernetwork, and $\text{Dir}(\alpha)$ denoting the Dirichlet distribution and r being the preference vector. During the optimization process, we update the hypernetwork parameter ϕ as follows:

$$\phi_{t+1} = \phi_t - \xi \nabla_{\phi} s(\mathcal{F}(\mathbf{x}_r), r), \quad (3)$$

where ξ is the step size, $s(\cdot)$ is the complete function. Upon completing the optimization process, we obtain ϕ^* , for each ray r , we derive the corresponding optimal solution $x_r = h(r, \phi^*)$.

In addition, for multi-task learning, our hypernetwork outputs the parameters θ of the target network $TN(\theta)$. In here, we obtain the loss function $\mathcal{L}(\cdot, \theta)$ by fitting the data sample and the parameter θ to the target network. This problem follows:

$$\phi^* = \arg \min_{\phi} \mathbb{E}_{r \sim \text{Dir}(\alpha)} s(\mathcal{L}(\cdot, \theta_r), r) \quad (4)$$

Here $\theta_r = h(r, \phi)$, the optimized process is similar to Formula (3).

Additionally, a complete function $s(\cdot)$ is employed to combine multiple objectives into a single objective for optimization. In previous studies, scalarization methods such as the linear or Chebyshev function have been used to identify optimal solutions

corresponding to a given preference vector. Moreover, other studies such as PHN-HVI utilize the hypervolume indicator to construct an objective function that guides the optimization process. This function is designed to maximize the hypervolume of the Pareto front, thereby directing the updates toward more optimal regions in the objective space.

3.3 Stein Variational Gradient Descent (SVGD)

Liu and Wang (2016) proposed a particle-based inference algorithm, SVGD, to approximate the target distribution by applying the gradient information in the updating process. SVGD starts at a set of initial points $\{x_i^0\}_{i=1}^n \in \mathbb{R}^d$ drawn by a prior distribution $p(x)$, which is pushed to the target points $\{x_i^*\}_{i=1}^n$ belonging to the target distribution $q(x)$, following the iterative:

$$\begin{aligned} x_i^{t+1} &\leftarrow x_i^t + \epsilon \phi^*(x_i^t), \forall i = 1, \dots, n, \\ \phi_k^* &= \arg \max_{\phi \in \mathcal{B}_k} \left\{ -\frac{d}{d\epsilon} \mathbf{KL}(q_{[\epsilon\phi]} \| p) \Big|_{\epsilon=0} \right\} \end{aligned} \quad (5)$$

Where, ϕ^* is an optimal transform function chosen to maximize the decreasing rate of the KL divergence between the distribution of particles and the target p , and $q_{[\epsilon\phi]}$ is defined the distribution of the updated particles, and \mathcal{B}_k is a unit ball of a reproducing kernel Hilbert space (RKHS) $\mathcal{H}_k^d := \mathcal{H}_k \times \dots \times \mathcal{H}_k$, \mathcal{H}_k is a Hilbert space associated with a positive definite kernel $k(x, x')$. The authors have shown that ϕ^* can be expressed as a linear operator:

$$\phi_k^* \propto \mathbb{E}_{x \sim q} [\mathcal{P}k(x, \cdot)] = \mathbb{E}_{x \sim q} [\nabla_x \log p(x) k(x, \cdot) + \nabla_x k(x, \cdot)] \quad (6)$$

4 Pareto Set Learning via Stein Variational Gradient Descent

4.1 Stein Variational Hypernetwork

In this study, we develop a novel method for Pareto set learning, which employs Stein Variational Gradient Descent to approximate the entire Pareto solution in Multi-objective learning problems. Furthermore, we explore the different gradient descents for learning in SVGD, providing a complete sense of learning the Pareto set. We name our method SVH-MOL.

We use hypernetwork to generate a set of initial particles, which is an advantage to flexibly changing the number of particles. Within the SVGD framework, each particle's movement is influenced by the repulsive forces from its neighboring particles. As the particle count increases, these repulsive interactions intensify, leading to faster convergence and a more diverse distribution of solutions across the Pareto front. Additionally, in multi-task learning, rather than training a separate network for every particle, the hypernetwork generates all necessary models on demand. This strategy not only streamlines the overall training process but also significantly reduces memory usage by enabling parameter sharing across tasks.

Building upon the previous study [Nguyen et al. \(2025\)](#), SVH-MOL needs to sample a set of an initial particle by using a hypernetwork. For the input of the hypernetwork, we use the predefined preference vector as a trade-off weight between objectives. Firstly, we sample n preference vectors r_i and fit them to the hypernetwork $\mathbf{h}(\cdot, \phi)$ to generate solutions $\{\mathbf{x}_{r_i}\}_{i=1}^n$. For a problem with m objectives, the objective functions are represented as $\mathcal{F}_i(\mathbf{x}_{r_i}) = [f_1(\mathbf{x}_{r_i}), \dots, f_n(\mathbf{x}_{r_i})]$, where \mathcal{F}_i is considered as a particle. The set of particles $\mathbf{F} = \{\mathcal{F}_i\}_{i=1}^n$ serves as the initialization set. We then iteratively advance this set of particles towards the Pareto front by applying the update rule in [Formula 3](#).

Stein Variational Gradient Descent plays a role in adjusting the direction of the gradient update and helps push the points away from each other, thereby enhancing the diversity of the Pareto front. Consequently, the following modifications will be applied to [Formula 3](#):

$$\phi_{t+1} = \phi_t - \xi \sum_{i=1}^n \sum_{j=1}^n \mathbf{g}(\mathcal{F}_i) \mathbf{k}(\mathcal{F}_i, \mathcal{F}_j) - \alpha \nabla_\phi \mathbf{k}(\mathcal{F}_i, \mathcal{F}_j) \quad (7)$$

where $\mathbf{k}(\mathcal{F}_i, \mathcal{F}_j)$ is kernel matrix. Gaussian kernel is used: $\mathbf{k}(\mathcal{F}_i, \mathcal{F}_j) = \exp(-\frac{1}{2h^2} \|\mathcal{F}_i - \mathcal{F}_j\|^2)$, h is bandwidth.

- When considering $\mathbf{g}(\mathcal{F}_i) \mathbf{k}(\mathcal{F}_i, \mathcal{F}_j)$, it is the driving force term that ensures the gradient update direction aligns with the intended path toward the optimal region.
- The second term, a repulsive force $\nabla_\phi \mathbf{k}(\mathcal{F}_i, \mathcal{F}_j)$ is responsible for maintaining diversity in the set of particles under consideration.

4.2 Controllable Pareto Set Learning

In traditional Stein Variational Gradient Descent (SVGD), a discrepancy measure known as the Stein discrepancy is used to quantify the difference between the current and target distributions. In a more recent study, [Ba et al. \(2021\)](#) introduced Mean Discrepancy Descent (MMD descent), a novel approach that replaces the original driving force in SVGD with one based on the Maximum Mean Discrepancy. Their work highlights a key limitation of SVGD, variance collapse, when approximating high-dimensional distributions. To address this issue, they modify the gradient update formulation, suggesting that for different problems, it may be beneficial to design a problem-specific driving force to guide particles toward better optimal solutions.

In the context of multi-objective learning, the Stein Variational Hypernetwork (SVH) is proposed to approximate the entire Pareto set. This approach leverages Stein's updating rule while utilizing a hypernetwork to generate candidate solutions. The idea of using a learnable hypernetwork to produce the Pareto set was introduced by [Tuan et al. \(2024\)](#), who proposed the Controllable Pareto Front Learning (CPF) framework. CPF trains a single hypernetwork whose parameters are optimized using principles from scalarization theory.

To enable controllable Pareto set learning in SVH, we incorporate three scalarization methods: Linear, TChebyshev, and Smooth TChebyshev. Each scalarization method modifies the driving force in SVH by computing the value $g(\mathcal{F})$ as the gradient

of the respective scalarization function. Each method induces a distinct optimization behavior, determined by the direction of its gradient. By experimenting with different scalarization operators, we aim to understand the impact of the repulsive term on SVH and how it contributes to the diversity and completeness of the resulting Pareto front.

Linear Scalarization Function (LS)

In multi-objective optimization, Linear Scalarization (LS) is a straightforward approach that combines multiple objectives into a single objective by computing a weighted sum. The gradient used for SVH is defined as:

$$g(\mathcal{F}_i) = \nabla \sum_{j=1}^m r_{i,j} f_j(x_{r_i}) \quad (8)$$

The weakness of this approach is that LS does not work well in non-convex problems. In these problems, the set of solutions lies on the convex envelope of the Pareto set. Therefore, the solution found is not aligned between the preference vector space and the objective space. In SVH, this disadvantage raises an interesting issue: whether the repulsive term can push the optimal solution into the non-convex region.

Tchebyshev Function (TCH)

The Chebyshev function is popular for many problems as it can produce the complete Pareto set in both non-convex and convex problems. It scalarizes multiple objectives by considering the maximum weighted deviation from the ideal point, which helps guide the optimization process even in regions where linear scalarization fails. The function is typically defined as:

$$g(\mathcal{F}_i) = \max_{j=1, \dots, m} r_{i,j} |f_j(x_{r_i}) - z_j^*| \quad (9)$$

where z^* is the ideal point. This formulation encourages solutions that minimize the worst-case deviation from the ideal point, making it well-suited for exploring non-convex regions of the Pareto front. However, the max operator introduces non-smoothness, which can hinder gradient-based optimization methods.

Smooth Tchebyshev Function (STCH)

To overcome the non-smooth nature of the standard Tchebyshev function, the Smooth Tchebyshev function [Lin et al. \(2024\)](#) replaces the max operator with a smooth approximation, such as the softmax or log-sum-exp function. A commonly used form is:

$$g(\mathcal{F}_i) = \frac{1}{\mu} \log \left(\sum_{j=1}^m \exp(\mu r_{i,j} |f_j(x_{r_i}) - z_j^*|) \right) \quad (10)$$

where $\mu > 0$ controls the smoothness. As $\mu \rightarrow \infty$, the function approaches the standard Tchebyshev function. This smooth approximation enables the use of

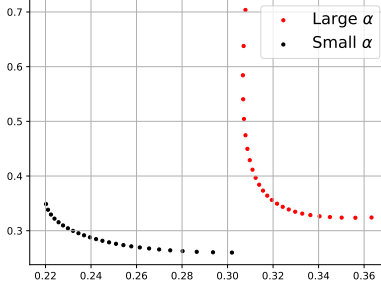


Fig. 2 Illustration of the change of Pareto front when changing α value.

gradient-based optimization while retaining the desirable properties of the Tchebyshov scalarization, such as its ability to explore non-convex regions and generate diverse solutions across the Pareto front.

4.3 Diversity-Promoting via Annealed SVH-MOL

In our optimization process, the gradient updates are influenced by two conflicting components. The first term acts as a driving force, guiding the solutions toward the optimal region. In contrast, the second term serves as a repulsive force, promoting diversity by preventing the solutions from collapsing onto one another along the Pareto front. This issue highlights the trade-off between convergence and diversity. While a Pareto front may exhibit good convergence, it does not necessarily guarantee diversity. In our experiments, we observed that prioritizing the repulsive term often leads to a Pareto set with poor optimality (Figure 2). In previous work, [Liu et al. \(2021\)](#) discussed the hyperparameter α in Formula (7), highlighting its influence on the diversity of the Pareto front. However, they were unable to effectively control this effect. In a recent study, [D'Angelo and Fortuin \(2021\)](#) also investigated this challenge and reported a variance collapse issue. They observed that particles in SVGD tend to collapse into a few local modes, a phenomenon strongly influenced by the initial particle distribution. To address this, they proposed an annealing schedule that gradually increases the weight of the driving force term. This strategy encourages the initial particles to spread across diverse regions at the beginning, guiding them toward a more diverse distribution throughout the optimization process.

$$\phi_{t+1} = \phi_t - \xi \sum_{i=1}^n \sum_{j=1}^n \gamma(t) \mathbf{g}(\mathcal{F}_i) \mathbf{k}(\mathcal{F}_i, \mathcal{F}_j) - \alpha \nabla_{\phi} \mathbf{k}(\mathcal{F}_i, \mathcal{F}_j) \quad (11)$$

Where $\gamma(t)$ is a coefficient that controls the influence of the driving term on the overall gradient update. [D'Angelo and Fortuin \(2021\)](#) varies $\gamma(t)$ in the interval $[0, 1]$ with an appropriate schedule; the process consists of two phases. The first is an exploratory phase, where a predominant repulsive force drives the points away from their initial positions, promoting broad coverage of the target distribution's support. The second is an exploitative phase, in which the driving force becomes dominant, guiding the points to concentrate around the various modes of the distribution.

Motivated by this approach, we propose a novel method for controlling the influence of the driving term. Rather than applying the scheduling function $\gamma(t)$ throughout the entire training process, we restrict its use to only the initial few epochs. Our rationale is that once the initial particles are sufficiently dispersed across different regions of the distribution, continued application of the pushing schedule in later epochs becomes unnecessary. Thus, our $\gamma(t)$ is formulated as:

$$\gamma(t) = \frac{\text{mod}(t, T_j)}{T_j}, T_{j+1} = \tau T_j \quad (12)$$

Here, we construct $\gamma(t)$ to vary over an initial long period of length T_0 , after which the length of each subsequent period T_i decreases according to a decay factor τ .

The motivation for our proposed approach stems from the observation that, within our framework, the SVGD gradient updates are highly sensitive to the parameters of the hypernetwork. Consequently, applying a strong repulsive force in the later training epochs can lead to instability in the convergence process, particularly near the optimal region.

5 Experiments

5.1 Evaluation Metrics

Mean Euclidean Distance (MED). [Tuan et al. \(2024\)](#) To evaluate the effectiveness of the controllable Pareto front, which means that the hypernetwork generates the optimal Pareto solution, aligning with the preference vector. We measure the error between the obtained Pareto solutions by the hypernetwork and the true Pareto solutions through calculating the mean of the Euclidean distance. The metric MED is defined as:

$$MED(\mathcal{F}^*, \hat{\mathcal{F}}) = \frac{1}{n} \left(\sum_{i=1}^n \|\mathcal{F}_i^* - \hat{\mathcal{F}}_i\|_2 \right) \quad (13)$$

Here $\mathcal{F}^* = \{\mathcal{F}_1^*, \dots, \mathcal{F}_n^*\}$ are the true Pareto solutions and the generated Pareto solutions $\hat{\mathcal{F}} = \{\hat{\mathcal{F}}_1, \dots, \hat{\mathcal{F}}_n\}$ corresponding to preference vector set $r \in \mathbb{R}_{>0}^m : \sum_i^m r_i = 1$. n is the number of rays that we consider for validation. A lower MED value indicates that the approximate solution is closer to the true Pareto front.

Hypervolume (HV). Hypervolume [Zitzler and Thiele \(1999\)](#) is a metric to figure out both convergence and diversity in the obtained solution. For some problems for which we lack the ground truth Pareto set, HV is an effective way to validate the quality of obtained solutions. The higher HV value reflects that the method is better. Given a set of n points $y = \{y^{(i)} | y^{(i)} \in \mathbb{R}^m; i = 1, \dots, n\}$ and a reference point $\rho \in \mathbb{R}^m$, the Hypervolume of y is measured by the region of non-dominated points bounded above by $y^{(i)} \in y$, then the hypervolume metric is defined as follows:

$$HV(y) = VOL \left(\bigcup_{y^{(i)} \in y, y^{(i)} \prec \rho} \Pi_{i=1}^n [y^{(i)}, \rho_i] \right) \quad (14)$$

where ρ_i is the i^{th} coordinate of the reference point ρ and $\Pi_{i=1}^n [y^{(i)}, \rho_i]$ is the operator creating the n -dimensional hypercube from the ranges $[y^{(i)}, \rho_i]$.

Spacing (SP). We employ the spacing metric [Schott \(1995\)](#); [Audet et al. \(2021\)](#) to observe the diversity in the Pareto solution set. This SP indicator captures the variation of the distance between solutions of a Pareto front approximation. A higher value is considered to be more diverse. SP is as follows:

$$SP(\hat{\mathcal{F}}) = \sqrt{\frac{1}{n-1} \sum_{i=1}^n (\hat{d} - d_i)^2} \quad (15)$$

where $d_i = \min_{i \neq j} \|\hat{\mathcal{F}}_i - \hat{\mathcal{F}}_j\|_1 \forall j = 1, \dots, n$, is the l_1 distance between a point $\hat{\mathcal{F}}_i \in \hat{\mathcal{F}}$, and the \hat{d} is the mean of all the d_i .

5.2 Multi-objective problems

In our study, we conduct extensive experiments to demonstrate our framework's effectiveness in many use cases. We compare the performance of our SVH-MOL with the baseline PSL methods: PHN-EPO, PHN-LS [Navon et al. \(2020\)](#), PHN-TCH (TChebyshev), and PHN-STCH (Smooth Tchebyshev) [Lin et al. \(2024\)](#).

5.2.1 Synthetic Problems

To validate the SVH-MOL's ability in towarding the optimal solution, we compare the MED on three synthetic tests: ZDT1, ZDT2 [Zitzler et al. \(2000\)](#). These ZDT problems have two objectives and 30 variables with a convex (ZDT1) and non-convex (ZDT2) Pareto-optimal set. In the optimization process, we train the hypernetwork with 20000 iterations and the hyperparameter $\alpha = 1e-5$. We compute MED value with the number of preference vectors for testing from 30 to 600 rays r_i .

In table 1, our SVH-MOL framework demonstrates that the performance of MED on synthetic tests outperform baseline methods. The main point is that SVH-MOL ensures convergence by following scalarization methods, while the repulsive term pushes the solutions toward better alignment between the preference vectors and the

| Rays | LS | Chebyshev | Smooth Chebyshev | SVH-LS (ours) | SVH-Chebyshev (ours) | SVH-SmoothChebyshev (ours) |
|-------------|-----------|-----------|------------------|------------------|----------------------|----------------------------|
| ZDT1 | | | | | | |
| 30 | 2.8184e-3 | 8.9748e-3 | 7.2197e-3 | 2.5042e-3 | 7.3183e-3 | 5.1942e-3 |
| 50 | 2.0595e-3 | 8.4050e-3 | 6.9985e-3 | 2.0582e-3 | 5.7081e-3 | 4.6705e-3 |
| 100 | 2.0372e-3 | 7.7228e-3 | 7.0542e-3 | 2.0300e-3 | 4.5971e-3 | 4.6375e-3 |
| 300 | 2.0403e-3 | 7.2580e-3 | 7.0194e-3 | 2.0212e-3 | 3.8971e-3 | 4.3241e-3 |
| 600 | 1.9957e-3 | 7.2239e-3 | 6.9931e-3 | 1.8053e-3 | 3.7411e-3 | 4.2328e-3 |
| ZDT2 | | | | | | |
| 30 | 7.0711e-1 | 6.0691e-3 | 2.4362e-3 | 7.0711e-1 | 5.1837e-3 | 2.0653e-3 |
| 50 | 7.0711e-1 | 6.1505e-3 | 2.0391e-3 | 7.0711e-1 | 4.7091e-3 | 2.0001e-3 |
| 100 | 7.0711e-1 | 5.9876e-3 | 2.0329e-3 | 7.0711e-1 | 4.2881e-3 | 2.0010e-3 |
| 300 | 7.0711e-1 | 6.0401e-3 | 2.0487e-3 | 7.0711e-1 | 4.2249e-3 | 1.9995e-3 |
| 600 | 7.0711e-1 | 5.9831e-3 | 2.0199e-3 | 7.0711e-1 | 4.1635e-3 | 1.9832e-3 |

Table 1 Comparison of MED values on ZDT1 and ZDT2 synthesis experiments.

| | LS | TCH | STCH | SVH-LS | SVH-TCH | SVH-STCH | A-SVH-LS | A-SVH-TCH | A-SVH-STCH |
|------|---------------|--------|---------------|---------------|---------------|---------------|---------------|---------------|---------------|
| RE21 | 0.8325 | 0.8330 | 0.8345 | 0.8322 | 0.8304 | <u>0.8332</u> | 0.8324 | 0.8299 | 0.8330 |
| RE22 | 0.5054 | 0.4961 | 0.4967 | 0.5538 | 0.5421 | 0.5317 | <u>0.5672</u> | 0.5679 | 0.5565 |
| RE23 | 0.0797 | 0.0755 | 0.0755 | 0.0822 | 0.2371 | 0.1091 | 0.0953 | 0.5538 | <u>0.4753</u> |
| RE24 | 1.1634 | 1.1630 | 1.1631 | 1.1636 | 1.1624 | 1.1597 | 1.1638 | 1.1626 | 1.1638 |
| RE31 | 1.3309 | 1.3308 | 1.3309 | 1.3309 | 1.3309 | 1.3309 | 1.3309 | 1.3309 | 1.3310 |
| RE32 | 1.3296 | 1.3296 | 1.3295 | <u>1.3297</u> | 1.3298 | <u>1.3297</u> | 1.3296 | <u>1.3297</u> | 1.3298 |
| RE33 | 1.0080 | 0.9902 | 0.9885 | 0.9281 | 1.0043 | <u>1.0101</u> | 0.9276 | 1.0022 | 1.0104 |
| RE34 | 0.6657 | 0.9870 | 0.9927 | 0.6657 | 0.9962 | <u>0.9983</u> | 0.6657 | 0.9964 | 0.9986 |
| RE35 | 1.0876 | 1.1445 | 1.1590 | 1.2113 | 1.1699 | 1.2963 | 1.1722 | 1.2737 | <u>1.2958</u> |
| RE36 | <u>1.0187</u> | 1.0181 | 1.0190 | 1.0176 | 1.0184 | 1.0178 | 1.0184 | 1.0180 | 1.0180 |
| RE37 | 0.7106 | 0.8258 | 0.8398 | 0.5938 | 0.8293 | 0.8373 | 0.8235 | 0.8320 | 0.8383 |

Table 2 Comparison of hypervolume values on real-world problems

Pareto-optimal points. In this experiment, we set a small value α to avoid the solution being pushed away from the optimal region. Moreover, in this result, we report only the vanilla SVH-MOL without the annealing schedule. Since the proposed annealing version of SVH-MOL encourages the discovery of a more diverse Pareto set, the resulting solutions may be suboptimal on synthetic problems.

5.2.2 Real-world Problems

We evaluate all methods on 11 RE problems (real-world engineering design problems) [Tanabe and Ishibuchi \(2020\)](#), which involve either two or three objectives. These problems present both convex and non-convex Pareto fronts, and some exhibit highly complex Pareto-optimal sets. Therefore, we aim to assess our framework on these benchmarks to evaluate its ability to approximate diverse and challenging Pareto fronts under realistic conditions.

In Table 2, SVH-MOL with the annealing schedule demonstrates superior performance, as A-SVH-{\LS, TCH, STCH} consistently achieves higher HV values compared to the baseline methods. Across each combination of SVH and a scalarization method, our proposed SVH-MOL generally obtains better results than the corresponding baselines.

Our SVH-MOL successfully captures the complete Pareto front, ensuring both convergence and diversity. In Figure 3, we visualize the Pareto front on RE37 with three objectives. The results highlight the effectiveness of our framework in handling complex Pareto sets. The Pareto fronts generated by A-SVH-{\LS, TCH, STCH} demonstrate better coverage compared to the baselines. Notably, in A-SVH-LS and A-SVH-TCH, the obtained Pareto sets cover most of the optimal solution space, unlike PHN-LS or PHN-TCH, which only capture a limited portion. This confirms the robustness and adaptability of our approach. Overall, SVH-MOL leverages the repulsive force term to promote diversity and preventing premature convergence.

5.3 Multi-task learning

In Multi-task learning, we compare our SVH-MOL performance with the baseline methods: PHN-LS, PHN-EPO, PHN-TCH, PHN-STCH, and PHN-HVI [Hoang et al. \(2023\)](#). The multi-task experiments consist of two benchmarks: image classification

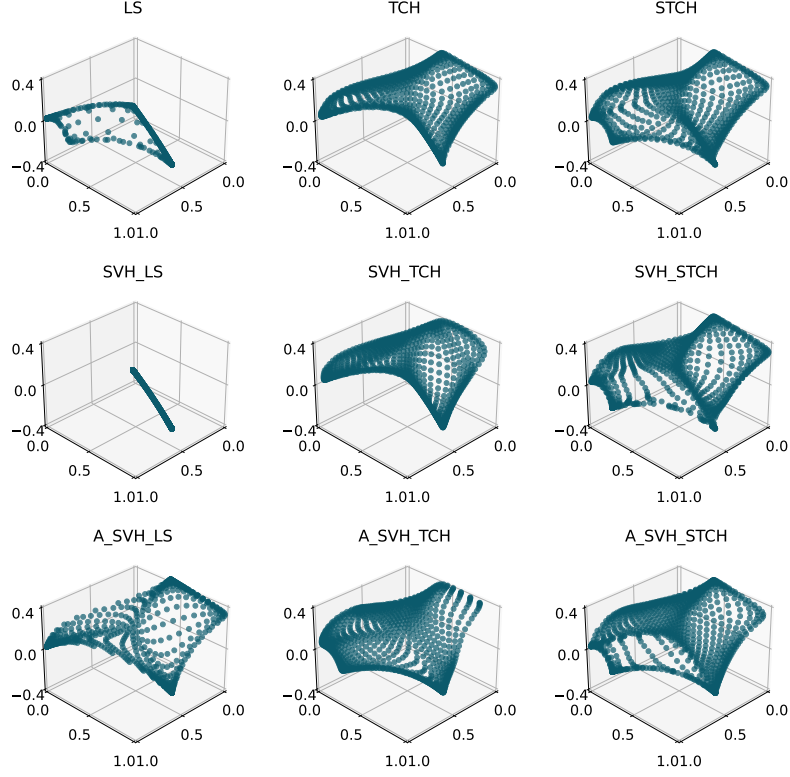


Fig. 3 Pareto fronts are generated on RE37.

(Multi-MNIST, Multi-Fashion, Multi-Fashion+ MNIST) [Lin et al. \(2019\)](#), and Multi-Output Regression (SARCOS) [Vijayakumar \(2000\)](#)

Image Classification

We train a hypernetwork to generate the complete set of parameters for a target network that performs image classification across three datasets: Multi-MNIST, Multi-Fashion, and Multi-MNIST+Fashion. Each dataset defines a two-objective multi-task learning problem, where the goal is to find a set of optimal Pareto solutions. Specifically, the tasks involve classifying two overlapping handwritten digits in Multi-MNIST, two overlapping fashion items in Multi-Fashion, and one handwritten digit and one fashion item in Multi-MNIST+Fashion. We use both the LSTM [Hochreiter and Schmidhuber \(1997\)](#) layer and the MLP layer in our core hypernetwork, and we employ a Multi-LeNet [Sener and Koltun \(2018\)](#) for the target network. In the training process, we set the number of preference vectors $n = 4$ and train for 500 epochs.

In table 3, our SVH-MOL achieves better performance than baseline approaches. In particular, our framework shows consistent and strong performance under various combinations of SVH and scalarizations, exceeding that of the baselines. While SVH-MOL clearly achieves a high HV (hypervolume) indicator, it exhibits poor diversity

| Method | Multi-MNIST | | Multi-Fashion | | Fashion-MNIST | |
|---------------------|---------------|-----------|---------------|---------|---------------|---------|
| | HV | Spacing | HV | Spacing | HV | Spacing |
| PHN-LS | 2.8056 | 0.0016 | 2.1292 | 0.0019 | 2.6915 | 0.0065 |
| PHN-Chebyshev | 2.8461 | 0.0081 | 2.1984 | 0.0159 | 2.7811 | 0.0324 |
| PHN-SmoothChebyshev | 2.8641 | 0.0028 | 2.1926 | 0.0082 | 2.7735 | 0.0211 |
| PHN-EPO | 2.7983 | 0.0059 | 2.1189 | 0.0114 | 2.6564 | 0.0139 |
| PHN-HVI | 3.0144 | 0.0072 | 2.3220 | 0.0136 | <u>2.9399</u> | 0.0095 |
| SVH-LS | 3.0147 | 7.3386e-5 | 2.1865 | 0.0002 | 2.9257 | 0.0002 |
| A-SVH-LS | 3.0263 | 0.0004 | 2.3421 | 0.0004 | 2.8963 | 0.0003 |
| SVH-TCH | 3.0952 | 0.0018 | 2.3820 | 0.0056 | 2.9291 | 0.0040 |
| A-SVH-TCH | <u>3.0946</u> | 0.0028 | 2.3761 | 0.0050 | 2.8772 | 0.0044 |
| SVH-STCH | <u>3.0709</u> | 0.0008 | <u>2.3891</u> | 0.0011 | 2.9556 | 0.0018 |
| A-SVH-STCH | 3.0641 | 0.0005 | 2.3915 | 0.0028 | 2.9081 | 0.0033 |

Table 3 Performance comparison across three datasets: Multi-MNIST, Multi-Fashion, Fashion-MNIST

(lower spacing indicator, Figure 4). We contend that this limitation is reasonable, given the difficulty of simultaneously achieving both convergence and diversity in the set of optimal solutions. Our SVH-MOL helps identify a better Pareto front while maintaining diversity among the solutions.

In this experiment, we compare performance between vanilla SVH-MOL and annealed SVH-MOL. These results indicate that A-SVH-MOL achieves better optimization compared to SVH-LS and A-SVH-LS, as it achieves more convergence and diversity. However, in other cases, the improvements are not clearly observed. We hypothesize that this phenomenon may stem from the sensitivity of the annealing factor, which strongly influences the parameter generation of the hypernetwork, specially in multi-task learning scenarios where the number of parameters is very large. In our experiments, the hypernetwork tends to be highly sensitive and is easily affected by annealing, which may explain why SVH-MOL does not consistently outperform the other methods.

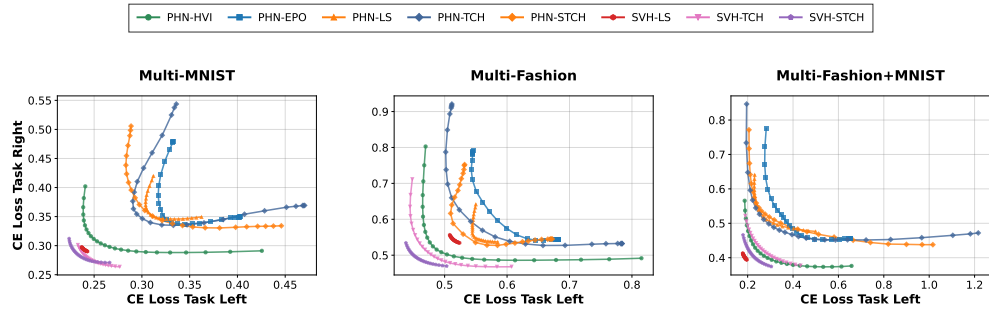


Fig. 4 Pareto fronts are generated by methods. We evaluate the result for 25 preference vectors.

| | Method | PHN-LS | PHN-TCH | PHN-STCH | PHN-EPO | PHN-HVI | SVH-LS | SVH-TCH | SVH-STCH | A-SVH-LS | A-SVH-TCH | A-SVH-STCH |
|--------|---------|--------|---------|----------|---------|---------|---------------|---------|----------|----------|-----------|------------|
| SARCOS | HV | 0.7149 | 0.7075 | 0.7098 | 0.7214 | 0.9556 | 0.9676 | 0.9613 | 0.9661 | 0.9548 | 0.9502 | 0.9576 |
| | Spacing | 0.0025 | 0.0100 | 0.0021 | 0.0029 | 0.0376 | 0.0283 | 0.0754 | 0.0302 | 0.0448 | 0.1233 | 0.0381 |

Table 4 Performance comparison across different methods on the SARCOS dataset

Multi-Output Regression.

The SARCOS dataset is a widely used benchmark for multi-task learning (MTL) and regression, particularly in robotics and control. We evaluate our model on a 7-task setup, where each task corresponds to predicting the torque of one of the seven robot arm joints. Each input is a 21-dimensional vector comprising joint positions (7), velocities (7), and accelerations (7). The output is a 7-dimensional vector of joint torques. The dataset contains 44,484 training and 4,449 test examples. We reserve 10% of the training set for validation.

Our results, presented in Table 4, show that SVH-MOL achieves superior performance compared to all baseline methods. Notably, A-SVH-MOL effectively promotes diversity in the learned Pareto set. These results demonstrate that SVH-MOL performs remarkably well on high-dimensional multi-objective problems, achieving superior outcomes in both optimization quality and solution diversity. This indicates that our framework offers a promising approach for approximating the Pareto front in many-objective optimization tasks.

5.4 Extended Results

5.4.1 Trade-off Between Convergence and Diversity

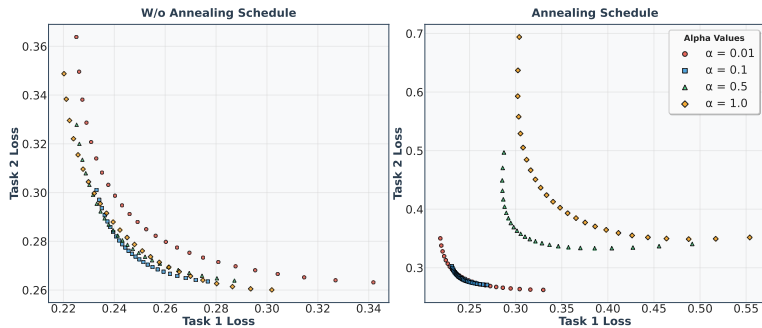


Fig. 5 Multi-MNIST: Comparative Analysis of Alpha Parameter.

In our research, we leverage the second term in the gradient update to encourage repulsion among particles, thereby enhancing diversity within the solution set. This naturally leads to a bi-objective scenario, where the objectives of convergence and diversity are inherently conflicting. In our approach, we emphasize diversity, which presents a significant challenge when the algorithm struggles to converge to the optimal solutions. The coefficient α in Formula 7 is introduced as a hyperparameter to promote

| Dataset | Cyclical SVH (C-SVH) | | | Annealed SVH (A-SVH) | | |
|---------|----------------------|--------|---------------|----------------------|---------------|---------------|
| | LS | TCH | STCH | LS | TCH | STCH |
| RE21 | 0.8322 | 0.8306 | 0.8319 | 0.8324 | 0.8299 | 0.8330 |
| RE22 | 0.5538 | 0.5542 | 0.5443 | 0.5672 | 0.5679 | 0.5565 |
| RE23 | 0.0815 | 0.1190 | 0.3940 | 0.0953 | 0.5538 | 0.4753 |
| RE24 | 1.1636 | 1.1511 | 0.1591 | 0.1638 | 0.1626 | 0.1638 |
| RE31 | 1.3310 | 1.3310 | 1.3309 | 1.3309 | 1.3309 | 1.3310 |
| RE32 | 1.3299 | 1.3298 | 1.3300 | 1.3296 | 1.3297 | 1.3298 |
| RE33 | 0.9296 | 1.0049 | 1.0138 | 0.9276 | 1.0022 | 1.0104 |
| RE34 | 0.9312 | 0.8683 | 0.8685 | 0.6657 | 0.9964 | 0.9986 |
| RE35 | 1.2479 | 1.2685 | 1.2963 | 1.1722 | 1.2737 | 1.2958 |
| RE36 | 1.0171 | 1.0158 | 1.0174 | 1.0184 | 1.0180 | 1.0180 |
| RE37 | 0.7103 | 0.8159 | 0.8324 | 0.8235 | 0.8320 | 0.8383 |

Table 5 Comparison of annealed SVH-MOL and cyclical SVH (C-SVH)

diversity. However, when varying α to study its impact on the shape and distribution of the Pareto set, the results are inconclusive. A similar issue has been observed in the study by Liu et al. (2021).

In Figure 5, our proposed annealing SVH-MOL exhibits distinct behavior as the value of α is varied. A higher α encourages greater diversity on the Pareto front, as reflected in its broader shape; however, this brings about a reduced convergence quality. This result demonstrates that our annealing SVH-MOL is more suitable for controlling the impact of the alpha value in the optimizing process.

5.4.2 Effect of the Annealing Schedule

In Table 5, we compare our annealed SVH-MOL with a baseline that employs a vanilla annealing schedule, where the annealing process is repeated with a fixed period. We refer to this baseline as C-SVH, representing cyclical SVH. These results demonstrate the effectiveness and stability of our framework, as it performs better in almost all experiments. Furthermore, the use of an annealing strategy enhances the performance of SVH, with C-SVH consistently achieving higher results compared to SVH without the annealing strategy.

6 Conclusion

In this paper, we introduce SVH-MOL, a novel framework that integrates Stein Variational Gradient Descent (SVGD) with hypernetwork-based techniques to efficiently approximate the entire Pareto set in multi-objective optimization. By incorporating an annealing schedule, our approach effectively balances convergence and diversity, addressing a key challenge in multi-objective learning. Extensive experiments on synthetic benchmarks and real-world multi-task learning problems demonstrate that SVH-MOL outperforms existing methods. These findings highlight the robustness and scalability of our method, paving the way for future advancements in controllable and efficient optimization techniques.

Acknowledgment

This research was funded by Vingroup Innovation Foundation (VINIF) under project code VinIF.2024.DA113. The authors also want to acknowledge the support of the Center for Environmental Intelligence at VinUniversity (project VUNI.CEI.FS_0007).

References

Marler, R.T., Arora, J.S.: Survey of multi-objective optimization methods for engineering. *Structural and Multidisciplinary Optimization* **26**(6), 369–395 (2004) <https://doi.org/10.1007/s00158-003-0368-6>

Craft, D., Halabi, T., Shih, H., Bortfeld, T.: Approximating convex pareto surfaces in multiobjective radiotherapy planning. *Medical Physics* **33**(9), 3399–3407 (2006) <https://doi.org/10.1118/1.2335486>

Milojkovic, N., Antognini, D., Bergamin, G., Faltings, B., Musat, C.: Multi-gradient descent for multi-objective recommender systems. arXiv preprint arXiv:2001.00846 (2019)

Jannach, D.: Multi-objective recommender systems: Survey and challenges. arXiv preprint arXiv:2210.10309 (2022)

Zaizi, F.E., Qassimi, S., Rakrak, S.: Multi-objective optimization with recommender systems: A systematic review. *Information Systems* **117**, 102233 (2023)

Sener, O., Koltun, V.: Multi-task learning as multi-objective optimization. *Advances in neural information processing systems* **31** (2018)

Crawshaw, M.: Multi-task learning with deep neural networks: A survey. arXiv preprint arXiv:2009.09796 (2020)

Lin, X., Yang, Z., Zhang, X., Zhang, Q.: Pareto set learning for expensive multi-objective optimization. *Advances in neural information processing systems* **35**, 19231–19247 (2022)

Nguyen, Q.-A.H., Tran, T.H.: High-dimensional bayesian optimization via random projection of manifold subspaces. In: *Joint European Conference on Machine Learning and Knowledge Discovery in Databases*, pp. 288–305 (2024). Springer

Zhang, Q., Li, H.: Moea/d: A multiobjective evolutionary algorithm based on decomposition. *IEEE Transactions on Evolutionary Computation* **11**(6), 712–731 (2007) <https://doi.org/10.1109/TEVC.2007.892759>

Chen, W., Zhang, X., Lin, B., Lin, X., Zhao, H., Zhang, Q., Kwok, J.T.: Gradient-based multi-objective deep learning: Algorithms, theories, applications, and beyond. arXiv preprint arXiv:2501.10945 (2025)

Liu, S., Johns, E., Davison, A.J.: End-to-end multi-task learning with attention. In: *Proceedings of the IEEE/CVF Conference on Computer Vision and Pattern Recognition*, pp. 1871–1880 (2019)

Kendall, A., Gal, Y., Cipolla, R.: Multi-task learning using uncertainty to weigh losses for scene geometry and semantics. In: *Proceedings of the IEEE Conference on Computer Vision and Pattern Recognition*, pp. 7482–7491 (2018)

Lin, X., Zhang, X., Yang, Z., Liu, F., Wang, Z., Zhang, Q.: Smooth tchebycheff scalarization for multi-objective optimization. arXiv preprint arXiv:2402.19078 (2024)

Chen, Z., Badrinarayanan, V., Lee, C.-Y., Rabinovich, A.: Gradnorm: Gradient normalization for adaptive loss balancing in deep multitask networks. In: *International Conference on Machine Learning*, pp. 794–803 (2018). PMLR

Yu, T., Kumar, S., Gupta, A., Levine, S., Hausman, K., Finn, C.: Gradient surgery for multi-task learning. *Advances in Neural Information Processing Systems* **33**, 5824–5836 (2020)

Lin, X., Zhen, H.-L., Li, Z., Zhang, Q.-F., Kwong, S.: Pareto multi-task learning. *Advances in neural information processing systems* **32** (2019)

Mahapatra, D., Rajan, V.: Multi-task learning with user preferences: Gradient descent with controlled ascent in pareto optimization. In: International Conference on Machine Learning, pp. 6597–6607 (2020). PMLR

Navon, A., Shamsian, A., Chechik, G., Fetaya, E.: Learning the pareto front with hypernetworks. arXiv preprint arXiv:2010.04104 (2020)

Hoang, L.P., Le, D.D., Tuan, T.A., Thang, T.N.: Improving pareto front learning via multi-sample hypernetworks. In: Proceedings of the Thirty-Seventh AAAI Conference on Artificial Intelligence and Thirty-Fifth Conference on Innovative Applications of Artificial Intelligence and Thirteenth Symposium on Educational Advances in Artificial Intelligence. AAAI'23/IAAI'23/EAAI'23. AAAI Press, ??? (2023). <https://doi.org/10.1609/aaai.v37i7.25953> . <https://doi.org/10.1609/aaai.v37i7.25953>

Deist, T.M., Grewal, M., Dankers, F.J.W.M., Alderliesten, T., Bosman, P.A.N.: Multi-Objective Learning to Predict Pareto Fronts Using Hypervolume Maximization (2021). <https://arxiv.org/abs/2102.04523>

Liu, X., Tong, X., Liu, Q.: Profiling pareto front with multi-objective stein variational gradient descent. In: Ranzato, M., Beygelzimer, A., Dauphin, Y., Liang, P.S., Vaughan, J.W. (eds.) *Advances in Neural Information Processing Systems*, vol. 34, pp. 14721–14733. Curran Associates, Inc., ??? (2021). https://proceedings.neurips.cc/paper_files/paper/2021/file/7bb16972da003e87724f048d76b7e0e1-Paper.pdf

Liu, Q., Wang, D.: Stein variational gradient descent: A general purpose bayesian inference algorithm. *Advances in neural information processing systems* **29** (2016)

Schaffer, J.D.: Multiple objective optimization with vector evaluated genetic algorithms. In: Proceedings of the First International Conference on Genetic Algorithms and Their Applications, pp. 93–100 (1984). Psychology Press

Deb, K., Jain, H.: An evolutionary many-objective optimization algorithm using reference-point-based nondominated sorting approach, part i: solving problems with box constraints. *IEEE transactions on evolutionary computation* **18**(4), 577–601 (2013)

Yang, X.-S.: Chapter 14 - multi-objective optimization. In: Yang, X.-S. (ed.) *Nature-Inspired Optimization Algorithms*, pp. 197–211. Elsevier, Oxford (2014). <https://doi.org/10.1016/B978-0-12-416743-8.00014-2> . <https://www.sciencedirect.com/science/article/pii/B9780124167438000142>

Steuer, R.E., Choo, E.-U.: An interactive weighted tchebycheff procedure for multiple objective programming. *Mathematical programming* **26**, 326–344 (1983)

Ha, D., Dai, A., Le, Q.V.: Hypernetworks. arXiv preprint arXiv:1609.09106 (2016)

Tuan, T.A., Hoang, L.P., Le, D.D., Thang, T.N.: A framework for controllable pareto front learning with completed scalarization functions and its applications. *Neural Networks* **169**, 257–273 (2024)

Zhuo, J., Liu, C., Shi, J., Zhu, J., Chen, N., Zhang, B.: Message passing stein variational gradient descent. In: International Conference on Machine Learning, pp. 6018–6027 (2018). PMLR

Ba, J., Erdogdu, M.A., Ghassemi, M., Sun, S., Suzuki, T., Wu, D., Zhang, T.: Understanding the variance collapse of svgd in high dimensions. In: International Conference on Learning Representations (2021)

D'Angelo, F., Fortuin, V.: Annealed stein variational gradient descent. arXiv preprint arXiv:2101.09815 (2021)

Duncan, A., Nüsken, N., Szpruch, L.: On the geometry of stein variational gradient descent. *Journal of Machine Learning Research* **24**(56), 1–39 (2023)

Ai, Q., Liu, S., He, L., Xu, Z.: Stein variational gradient descent with multiple kernels.

Cognitive Computation **15**(2), 672–682 (2023)

Liu, X., Tong, X., Liu, Q.: Profiling pareto front with multi-objective stein variational gradient descent. Advances in neural information processing systems **34**, 14721–14733 (2021)

Nguyen, M.-D., Dinh, P.M., Nguyen, Q.-H., Hoang, L.P., Le, D.D.: Improving pareto set learning for expensive multi-objective optimization via stein variational hypernetworks. Proceedings of the AAAI Conference on Artificial Intelligence **39**(18), 19677–19685 (2025) <https://doi.org/10.1609/aaai.v39i18.34167>

Zitzler, E., Thiele, L.: Multiobjective evolutionary algorithms: a comparative case study and the strength pareto approach. IEEE transactions on Evolutionary Computation **3**(4), 257–271 (1999)

Schott, J.R.: Fault tolerant design using single and multicriteria genetic algorithm optimization. PhD thesis, Massachusetts Institute of Technology (1995)

Audet, C., Bégin, J., Cartier, D., Le Digabel, S., Salomon, L.: Performance indicators in multiobjective optimization. European journal of operational research **292**(2), 397–422 (2021)

Zitzler, E., Deb, K., Thiele, L.: Comparison of multiobjective evolutionary algorithms: Empirical results. Evolutionary Computation **8**(2), 173–195 (2000) <https://doi.org/10.1162/106365600568202> <https://direct.mit.edu/evco/article-pdf/8/2/173/1493199/106365600568202.pdf>

Tanabe, R., Ishibuchi, H.: An easy-to-use real-world multi-objective optimization problem suite. Applied Soft Computing **89**, 106078 (2020)

Vijayakumar, S.: The SARCOS Dataset. Accessed: 2023-03-09 (2000). <http://www.gaussianprocess.org/gpml/data>

Hochreiter, S., Schmidhuber, J.: Long short-term memory. Neural Comput. **9**(8), 1735–1780 (1997) <https://doi.org/10.1162/neco.1997.9.8.1735>